CBPF-NF-026/04

The CRISP package for intermediate- and high-energy photonuclear reactions

A. Deppman[1], S.B. Duarte[2], G. Silva[1], O.A.P. Tavares[2], S. Anéfalos[1], J.D.T. Arruda-Neto[1,3], and T. E. Rodrigues[1]

1) Instituto de Física, Universidade de São Paulo CP66318 - CEP 05315-970 - São Paulo - SP, Brazil.

2) Centro Brasileiro de Pesquisas Física CEP 22290-180 - Rio de Janeiro - RJ, Brazil

3) Universidade de Santo Amaro CEP 04829-300,Santo Amaro - SP, Brazil

Abstract

The two-step process that characterize the intermediate and high energies photonuclear reactions (between 40 MeV and 4 GeV) has been successfully described by Monte Carlo calculations. Recently, a new class of codes capable to perform those calculations according to a more realistic method has been developed, improving the possibilities for simulating the reactions in more details. In this work we present the CRISP package (standing for Rio-São Paulo Collaboration), which is a coupling of the Multi Collisional Monte Carlo (MCMC) and the Monte Carlo for Evaporation-Fission (MCEF) codes. The first one describes the intranuclear cascade process, while the second one is dedicated to the evaporation/fission competition step. Both codes have already shown to be useful for calculating several features of different nuclear reactions. The CRISP code, coupling these two softwares, represents a good tool to describe the complexes characteristics of the nuclear reactions, and opens the opportunity for applications in quite different fields, such as studies of hadron physics inside the nucleus, specific nuclear reactions, spallation and/or fission processes initiated by different probes, and many others.

Pacs numbers: 23.23.+x, 56.65.Dy

I. INTRODUCTION

The Monte Carlo approach for describing the nuclear reactions at intermediate and high-energy (between 40 MeV and 4 GeV) regions has shown to be a successful one [1–4]. At these energies, the nuclear reactions can be understood as a two-step process, where the first one is the so-called intranuclear cascade, which leads to the formation of an excited thermalized residual nucleus, and the second step, where the competition between particle evaporation and the fission process takes place.

Monte Carlo method must be seen as a complementary method for understanding nuclear reactions. Statistical and phenomenological models also allow the calculation of the main feature of the intranuclear and evaporation processes [4–8]. The main advantage of the Monte Carlo method presented in this work is the inclusion of a detailed description of the elementary reactions during the intranuclear cascade and the evaporation phase (including fission) rendering this method usefull for photonuclear reactions in actnide nuclei.

The first codes developed using the Monte Carlo approach [9–11] consider the intranuclear cascade as an unrealistic sequence of single-nucleon tracks, along which the possible nucleon-nucleon interactions are considered, while all the other nucleons stand as spectators. Due to this restriction, some well known physical phenomena, as the Pauli blocking of final states produced during the intranuclear cascade, and the local density fluctuations must be introduced by rather indirect, and again unrealistic, methods. Nowadays, a new approach is emerging, where the intranuclear cascade is considered as a sequence of elementary interactions between the nucleons and other particles (as mesons, nucleonic resonances and exotic particles) which is ordered according to the causal relation among all possible events, keeping a realistic time-dependent evolution of the nuclear configuration[3].

This method is also employed in Monte Carlo calculations for high-energy heavy-ions collisions [2, 12], where the Quantum Molecular Dynamic model is usually adopted. The present work, however, is focused on photonuclear reactions, which presents some distinct features respect to heavy-ions collisions, since the electromagnetic probe keeps the nuclear structure almost unchanged in the very first stage of the intranuclear cascade. In what follows we are referring specifically to photonuclear reactions, unless we explicitly state

the contrary.

Although this modern approach is much closer to the real physical evolution of the cascade process, many problems have shown up, leading also to unphysical results such as negative excitation energies of the residual nucleus formed at the end of the cascade, or occupation number of the fermionic states higher than unit, in a clear violation of the Pauli Principle[13, 14]. All these problems are addressed in this work, where we present the CRISP (Rio - São Paulo Collaboration) package for nuclear reactions calculations.

This paper is organized as follows. In section II The Monte Carlo approach is reviewed, where we describe in more details how the calculations are performed, and the advantages and problems related to this method. In section III we present the CRISP package, where the main features of our calculation method are remarked, and how many of the problems discussed in section II are solved. In section IV some results are presented from the CRISP package. Finally, section V presents the conclusions, where we discuss the main features of our package.

II. THE MONTE CARLO APPROACH

The Monte Carlo calculations for nuclear reactions are generally based on the fact that at intermediate and high energies the reactions can be understood as a two-step process. Initially, a fast sequence of elementary nucleon-nucleon interactions transfer the energy from the incident particle to a small number (compared to the mass number) of nucleons, in a process known as intranuclear cascade. This process finishes when the energy of each and every particle inside the nucleus is below its separation energy. At this point, an excited residual nucleus is formed, and after a while the total energy is thermalized, i.e., it is distributed among practically all the nucleons of the nucleus.

After this stage, the slow process of evaporation of secondary particles initiates a stochastic competition with the fission process, where the relevant quantities are the branching ratios for each decaying channel. Usually the most important processes considered in this stage are the emission of neutrons and, for heavy nuclei, fission.

The classical Monte Carlo calculations[9–11] consider the intranuclear cascade as a sequence of individual particle events along their tracks. These sequences are included in

the cascade with the unphysical hypothesis that all the other particles inside the nucleus may be treated as static objects. Although many interesting results have been obtained, it is difficult to describe the entire nuclear reaction, including most of the possible channels, either qualitatively or quantitatively. In fact, these models do not take into account the local density fluctuations during the cascade process, or the variability of the occupation numbers of levels below the Fermi level during the reaction. However, these characteristics of the nuclear reactions can, indeed, have strong influences on some results such as, for instance, excitation energy of the residual nucleus and the secondary particle multiplicities.

Recently, a new class of Monte Carlo models have been developed[3, 13], where the intranuclear cascade process is performed on a realistic time-sequence approach in which all particles inside the nucleus can participate in the cascade, and the semi-classical trajectory of all particles are followed during the process. In this way, nuclear density fluctuations are naturally taken into account during the cascade, and also the variations of the occupation number of each single particle level are considered as a function of time. In fact, although these new models have much more realistic mechanisms to simulate the nuclear reactions, they still give rather unphysical results such as negative excitation energy for the residual nucleus obtained at the end of the cascade and level occupation number greater than unit, which clearly violates the Pauli Principle[13, 14].

On the other hand, the slow process of competition between evaporation and fission was usually oversimplified by the assumption that only neutron evaporation is the relevant process in the comparison with the fission probabilities. However, it has been recently shown that this assumption is not correct[15], even for heavy nuclei, for which fissilities are close to 100%. Only with the inclusion of the evaporation of protons and alpha-particles it is possible to predict almost correctly the values for fissilities of actinides and pre-actinides[16]. This model for evaporation/fission and the corresponding software are described in Ref. [17].

The MCMC code for the intranuclear cascade process [3], and the MCEF code for the evaporation/fission competition process[18], which incorporate most of the characteristics discussed above, are coupled to each other in one single package called CRISP, which includes also some additional improvements. The interface between the MCMC and

MCEF is performed by a simple routine which takes the values of mass, atomic numbers and excitation energy for the compound nucleus obtained at the end of the MCMC run, and passes them as input to the MCEF code, which performs the evaporation/fission competition process.

III. THE CRISP PACKAGE

In this section we describe the CRISP package, emphasizing the improvements introduced into the original MCMC and MCEF codes. As discussed above, one critical issue in the Monte Carlo calculations for nuclear reactions at intermediate and high energies is the correct simulation of the Pauli blocking effect. The most recent codes allow a more realistic modeling of this mechanism, since at any time the energies of all nucleons inside the nucleus are known, and therefore the occupation number of each discrete single-particle level is also known. This was not true in old, classical Monte Carlo calculations, where each track was followed up to the moment the particle leaves the nucleus, while all the other particles are considered as standing at rest.

However, this advantage of the modern codes is not yet fully incorporated. In fact, the variations of level occupation number during the intranuclear cascade were not considered in a realistic way, and the Pauli Principle is usually incorporated by means of statistical mechanisms which lead to violations of this principle clearly seen in the occupation numbers of low energy levels, in negative excitation energies of the residual nucleus and in the so-called nuclear boiling[13, 14]. These problems result in some difficulties such as the impossibility of keeping the nucleus as a stable system during long time, even if it is not perturbed by any external agent, such as an incident particle, incorrect excitation energy of the residual nucleus, secondary multiplicities and spectra, in disagreement with experimental data.

In the CRISP model, we introduced the time-sequence characteristics of the MCMC code[3] and the evaporation/fission competition process of the MCEF model[17, 18]. In addition, we improved the code by taking into account:

- the excitation of nucleonic resonances heavier than the Δ-resonances;
- the initial nuclear ground state construction according to the Fermi Model and Pauli

Principle;

- a more realistic Pauli blocking mechanism;
- the quasi-deuteron channel for photoabsorption;
- adaptation of the evaporation/fission competition model from the MCEF code[18] to coupling with the MCMC code[3] after the improvements referred above. Such modifications are described below to some details.

A. Nucleonic resonances

At intermediate energies, the excitation of nucleonic resonances is the major mechanism in the nuclear reaction, mainly for photonuclear reactions. In fact, it is evident in the photoabsorption cross section the structures due to resonant photoabsorption.

These resonances play a fundamental role also in the subsequent intranuclear cascade, since they propagate inside the nucleus and can decay into several different channels which determines how the intranuclear cascade will evolve.

The only nucleonic resonance that could be excited by photon absorption in the original MCMC code was the Delta one. We included the other two major resonances in the photoabsorption, namely the D_{13} and F_{35} resonances in order to better describe the photo-reactions between 500 and 1000 MeV[19]. The possible decaying channels and their respective probabilities, for each resonance, are

$$\begin{aligned}
N^*(P_{33}) &\rightarrow n + \pi \ (100\%)\,; \\
N^*(D_{13}) &\rightarrow n + \pi \ (50\%)\,; \\
N^*(D_{13}) &\rightarrow n + \Delta + \pi \rightarrow n + \pi + \pi \ (25\%)\,; \\
N^*(D_{13}) &\rightarrow n + \rho \rightarrow n + \pi + \pi \ (25\%)\,; \\
N^*(F_{35}) &\rightarrow n + \pi \ (15\%)\,; \\
N^*(F_{35}) &\rightarrow \Delta + \pi \rightarrow n + \pi + \pi \ (25\%)\,; \\
N^*(F_{35}) &\rightarrow n + \rho \rightarrow n + \pi + \pi \ (60\%)\,.
\end{aligned} \tag{1}$$

These resonances are described by Breit-Wigner's formulae

$$\sigma = \sigma_o \frac{\left(\frac{\Gamma}{2}\right)^2}{(E - E_o)^2 + \left(\frac{\Gamma}{2}\right)^2}\,, \tag{2}$$

where E_o is the resonance mass, Γ is its width, and σ_o is its maximum cross section value. These parameters are determined for each resonance by a fitting procedure to the cross section data for proton and neutron targets [19]. The resonance characteristics can be modified by nuclear effects such as Fermi motion and Pauli blocking. These effects are naturally accounted for by the CRISP calculation, since the photoabsorption cross section is always calculated at a reference frame in which the absorbing nucleon is at rest. Therefore, a Lorentz transformation is performed, modifying in this way the incident photon energy. The Pauli blocking mechanism, which is described below, also contributes to modifications of the resonances, as it may block the decaying channels of the resonances. The distribution of the decaying particle is determined by imposing energy and momentum conservation and is considered isotropic in the CM frame.

Once a resonance is created, it propagates inside the nucleus, as described in [3]. The mean-life time of each resonance is calculated according to the Uncertainty Principle, i.e.

$$\Gamma\tau = \hbar\,, \tag{3}$$

where Γ is the resonance width, and τ is its mean-life time. Also, if this particle decays through a channel in which a ρ meson is created, it can also propagate before decaying into two pions.

B. Initial nuclear ground state and Pauli blocking mechanism

The Pauli blocking mechanism is accounted for by dividing the phase-space into cells. The cell corresponds to a quantum-level, which is determined according to the Fermi gas model, where the momentum components, p_x, p_y and p_z, are the good quantum numbers. In this approach, due to spin and isospin degrees-of-freedom of the nucleons, we can place up to four nucleons on each level.

The Pauli blocking mechanism consists in the verification, after each possible interaction between different particles in the nucleus, if there is a cell available for the final

state particles. If all the secondaries can be placed at the correct levels, the interaction is allowed, otherwise it is blocked. This process must be performed at every stage of the cascade, and also in the construction of the initial ground state nucleus.

In fact, in the Monte Carlo models, the initial nucleus configuration is usually chosen randomically, without verifications for possible violation of the Pauli Principle. In our code we construct the ground state in a deterministic way, by filling all available levels from the bottom to the Fermi level, in accordance with that Principle. The energy gap, ΔE, between the levels are obtained according to the expression

$$\Delta p = \frac{\hbar}{2\Delta x}\,, \tag{4}$$

where Δx is the nucleon position uncertainty, and Δp is the momentum uncertainty.

The quantum levels are characterized by the momentum components $p_i = n_i \Delta p$, with n_i being an integer, and $i = x, y, z$. Also, the total momentum is given by

$$p^2 = p_x^2 + p_y^2 + p_z^2 = (n_x^2 + n_y^2 + n_z^2)(\Delta p)^2 = n^2(\Delta p)^2\,, \tag{5}$$

where n must be an integer. The condition that n and n_i, for any i, must be integers restricts the number of possible states. The possible quantum levels are then characterized by the triplets n_x, n_y, n_z, which must satisfy the condition (5).

Another restriction to the value of Δp is the nuclear potential, V_0, which is related to the Fermi energy E_F by $V_0 \approx E_F + 7\text{MeV}$, while E_F is calculated according to the Fermi gas model. For the ^{208}Pb nucleus, for instance, this leads to $\Delta p = 28.57\text{MeV/c}$ for protons and $\Delta p = 26.45\text{MeV/c}$ for neutrons. These results, together with Heisenberg's Principle, give $\Delta x \sim 5.5\text{fm}$, a value which is compatible with the nuclear dimension. This result is an indication of the self-consistence of our model.

The effective mass of the nucleon, m^*, depends on its momentum according to

$$\sqrt{p^2 + m_0^2} - V_0 \equiv \sqrt{p^2 + m^{*2}}\,. \tag{6}$$

The mean effective mass, calculated as an average over the ground state momentum distribution, is $\bar{m^*} = 0.951 m_0$, a value in good agreement with that reported in [20], $m^* = (0.953 \pm 0.002) m_0$.

The Pauli exclusion principle is incorporated into our model by ensuring that at any step of the intranuclear cascade calculation the number of nucleons at any level n_x, n_y, n_z will be not greater than the limit allowed by that principle.

One of the main advantages of this method, compared to those adopted by similar approaches[13, 14, 21], is the elimination of unphysical results such as the violation of the Pauli Principle, or the spurious depletion of the Fermi-sphere, which shows up in the form of "spontaneous nuclear boiling"[14], leading to problems such as the incorrect calculation of the occupation number and secondary multiplicities, the impossibility of keeping the nucleus stable during long times (or many cascade iterations), and the use of arbitrary stopping-time parameters to finish the calculation of the cascade process, which, nonetheless, gives rise to events of negative excitation energy.

With the CRISP package we eliminate all those undesirable effects and their unphysical consequences. Furthermore, our approach propitiates a more realistic description of the cascade process, allowing the re-population of the Fermi-sphere by any nucleon inside the nuclear volume during the intranuclear cascade. With these improvements, we established a physical, energetic criteria for stopping the intranuclear cascade calculation, i.e., when all the bound nucleons do not have sufficient energy to escape from the nucleus. A more comprehensive discussion is given in [22].

C. Quasi-Deuteron

The quasi-deuteron mechanism is included to take into account the possibility of two-body correlation effects during the photoabsorption. This mechanism is relevant for photon energies between ~ 40 MeV and ~ 140 MeV. We adopted the Levinger's model[23] to calculate the cross section, σ_{qd}, for the quasi-deuteron absorption of a photon of energy ω, which is given by

$$\sigma_{qd}(\omega) = \frac{NZ}{A}\frac{2\pi}{v}\frac{1-\gamma r_o}{\gamma(\gamma^2+k^2)}\sigma_d(\omega)\,, \tag{7}$$

where v is the nuclear volume, k is the proton-neutron relative momentum, γ is related to the proton-neutron scattering phase-shift, δ, through $\gamma = -k\,cot\delta$, σ_d is the deuteron photodisintegration cross section, and r_o is the effective scattering length. The quantities A and Z are the nuclear mass and atomic numbers, respectively, and $N = A - Z$.

The factor

$$\frac{1-\gamma r_o}{\gamma(\gamma^2+k^2)} \tag{8}$$

in the above expression is understood as the probability of finding a correlated proton-

neutron pair to form a quasi-deuteron[24], which depends on the relative momentum of the proton and neutron.

D. Evaporation-fission competition

The evaporation-fission competition process is performed following the routine used in the MCEF code [17, 18], but including a few modification in the calculation of the level density parameters, which have been used as free parameters to fit the experimental data.

IV. RESULTS

In this section we show a few results obtained with the CRISP package. We note that the CRISP code is the result of a coupling of the MCMC with MCEF codes, and therefore it inherits all the elementary reactions, particles and processes already incorporated into those codes (see references [3, 17] for more details), also including strangeness production [25]. In addition, as described in Section III.A, it includes barionic resonances heavier than Δ in the photoabsorption process, meson ρ formation by decaying resonances and photon hadronization, and two-pion resonance decay. Almost all parameters of the code are determined from well-known theoretical or experimental works, and they are exactly the same as those used in the MCMC and MCEF codes [3, 18].

As described above, one of the most common problems we met frequently in Monte Carlo calculations of nuclear reactions is related to the correct introduction of the Pauli blocking mechanism. This problem has been solved in the CRISP package, as we have discussed above. Some of the consequences are shown in figure 1, where we plotted the occupation number for levels at different energies as calculated by the present code (full line) and the INC code (dashed line)[13]. As we can observe, while the INC model violates the Pauli Principle by allowing more than one fermion at the same level, the CRISP results does not give rise to occupation number greater than unit. This reflects a better approach to Pauli blocking mechanism in our package.

The Pauli Blocking mechanism can be effectively tested by applying it to photonuclear reactions in the quasi-deuteron region of photonuclear absorption. In fact, most of the secondaries produced in the absorption of a photon by a quasi-deuteron pair has energy

below or close to the Fermi energy, therefore the probability of blocking these particles is quite high. We calculated the photoabsorption cross section per nucleon in the quasi-deuteron region, a quantity which is sensitive to the model adopted for the Pauli blocking mechanism. In Figure 2 we show the results of our calculation for several nuclei. The good agreement with the experimental data indicates that the CRISP code correctly calculates the most important features of Pauli blocking and quasi-deuteron mechanisms. As the quasi-deuteron cross section is proportional to NZ/A, the normalized cross section shown in Figure 2 is proportional to NZ/A^2, which is approximately 0.24 for all nuclei studied. For this reason the normalized cross section is approximately equal for those nuclei.

The neutron multiplicity at the end of the nuclear reaction, on the other hand, allows us to test the performance of the CRISP calculations for the entire nuclear reaction, i.e. including both the intranuclear cascade and evaporation/fission competition processes, since the calculation strongly depends on the characteristics of both steps of the reaction. In Figure 3 we present our results for neutron multiplicities in the quasi-deuteron region. The agreement between calculated and experimental data is another evidence of the correctness of the CRISP approach for simulating nuclear reactions.

Finally, with the inclusion of the most relevant nucleonic resonances, we can calculate the photoabsorption and photofission cross sections. One of the difficulties we faced with most of the Monte Carlo calculations is the evaluation of the fission properties of different nuclei inside one single model. Fissility of actinide and preactinide nuclei are already very different, due to the strong variations of the fission barriers and level-density parameters, thus making difficult to calculate correctly the photofission cross section, which is very sensitive to these parameters. With the CRISP code we succeeded to perform the calculation of the photofission cross sections for various actinide and preactinide nuclei. In Figure 4 we present the results for Pb and Bi targets, and compare them with experimental data. In Figure 5 we show the results for a number of actinide nuclei together with the experimental data.

The good agreement found for all nuclei in the energy range from 0.15 up to 1.2 GeV is a strong evidence that the CRISP code calculates correctly most of the reaction mechanisms which are important during the entire reaction process. We remark that the photofission result is dependent on complex processes. The reaction initiates by the

photoabsorption mechanism, evolves through resonance propagation and decay, intranuclear cascade process, and formation of an excited residual nucleus. This nucleus, then, initiates the evaporation-fission process, and from the competition between the different channels opened during this process, we obtain the photofission cross section. The photofission cross section result is, thus, a consequence of the correct description of the different processes with take place during the nuclear reaction.

V. CONCLUSIONS

In this work we present the CRISP package for intermediate and high energies nuclear reactions. This package was constructed by the coupling of the MCMC[3] and MCEF[18] codes, with the introduction of some improvements, such as a better Pauli blocking mechanism, the formation of a nuclear ground state according to the Fermi model and in accordance to the Pauli Principle, the introduction of the most relevant resonant excitation and de-excitation for nucleon photoabsorption, and the quasi-deuteron mechanism of nuclear photoabsorption.

We describe some of the consequences resulting from these modifications, and present a few results in order to illustrate the possible applications to which this package can be used. We calculate the photofission cross section for various different actinide and preactinide nuclei at energies going from 40 MeV up to 1.2 GeV, and compare them with experimental data. We calculate the neutron multiplicities for different target nuclei, and show that they are in good agreement with experimental results. Also, we discuss the effects of a correct Pauli blocking calculation on more fundamental aspects as, for instance, the occupation number of levels below the Fermi energy at the end of the cascade process.

All these results show that the CRISP code is an important and reliable tool for calculating the characteristics of photonuclear reactions for different nuclei and incident energies.

VI. ACKNOWLEDGMENT

The authors acknowledge the Brazilian agencies FAPESP and CNPq for supporting of this work.

VII. REFERENCES

[1] Filges D., et al., 2001 Eur. Phys. J. A 11, 467.

[2] Bass S.A. et al., 1988 Progr. Partic. Nucl. Phys. 41, 255.

[3] Gonçalves M., de Pina S., Lima D. A., Milomen W., Medeiros E. L., and Duarte S. B. 1997 Phys. Lett. B 406, 1.

[4] Kikuchi K. and Kawai M. in *Nuclear Matter and Nuclear Reactions*, North-Holland Pub Comp., Amsterdam, 1968.

[5] Campi X. and Hüfner, 1981 Phys. Rev. C 24, 2199.

[6] Deppman A.,Arruda-Neto J.D.T., DeSanctis E. and Bianchi N., 1996 Nuovo Cim. A 109, 1197.

[7] Deppman A. and Arruda-Neto J.D.T., 1999 Eur. Phys. J. A 6, 107.

[8] Tavares O.A.P., Duarte S.B., Deppman A., Likhachev V.P., 2004 J. Phys. G Nucl. Partic.30, 377.

[9] Bertini H. W. 1963 Phys. Rev. 131, 1801.

[10] Barashenkov V. S., Gereghi F. G., Iljinov A. S., Jonsson G. G. and Toneev V. D. 1974 Nucl. Phys. A 231, 462.

[11] Yariv Y. and Fraenkel Z. 1981 Phys. Rev. C 24, 488.

[12] Belkacem M. et al., 1988 Phys. Rev. C 58, 1727.

[13] Cugnon J., Volant C., and Vuillier S. 1997 Nucl. Phys. A 620, 475.

[14] Boudard A., Cugnon J., Leray S., and Volant C. 2002 Phys. Rev.C 66, 044615.

[15] Deppman A., Tavares O. A. P., Duarte S. B., de Oliveira E. C., Arruda-Neto J. D. T, de Pina S. R., Likhachev V. P., Rodriguez O., Mesa J. and Gonalves M. 2001 Phys. Rev. Lett. 87, 182701.

[16] Deppman A., Tavares O. A. P., Duarte S. B., Arruda-Neto J. D. T, Gonalves M., Likhachev

V. P. and de Oliveira E. C., 2002 Phys. Rev. C 66, 067601.

[17] Deppman A., Tavares O. A. P., Duarte S. B., Arruda-Neto J. D. T, Gonalves M., Likhachev V. P., Mesa J., de Oliveira E. C., de Pina S. R. and Rodriguez, O. 2003 Nucl. Instrum. Methods Phys. Res. B 211, 15.

[18] Deppman A., Tavares O. A. P., Duarte S. B., de Oliveira E. C., Arruda-Neto J. D. T., de Pina S. R., Likhachev V. P., Rodriguez O., Mesa J. and Gonalves M. 2002 Comput. Phys. Commun. 145, 385.

[19] Deppman A., Bianchi N., de Sanctis E., Mirazita M., Muccifora V. and Rossi P. 1998 Il Nuovo Cim. A 111, 1299.

[20] Garcia Canal C. A., Santangelo E. M. and Vucetich H. 1984 Phys. Rev. Lett. 53, 1430.

[21] Cugnon J. and Henrotte P. 2003 Eur. Phys. J. A 16, 393.

[22] Rodrigues T.E. et al., 2004 Phys. Rev. C 69, 064611.

[23] Levinger J.S., 1951 Phys. Rev. 84, 43.

[24] Chadwick M.B. et al, 1991 Phys. Rev. C 44, 814.

[25] de Pina S., de Oliveira E. C., Medeiros E. L., Duarte S. B. and Gonçalves M. 1998 Phys. Lett. B 434, 1.

[26] Leprêtre A., Beil H., Bergère R., Carlos P., Fagot J., De Miniac A. and Veyssière A. 1981 Nucl. Phys. A 367, 237.

[27] Leprêtre A., Beil H., Bergère R., Carlos P., Fagot J. and Veyssière A., 1982 Nucl. Phys. A 390, 221.

[28] Bellini V. , 1983 Lett. Nuovo Cimento 36, 587.

[29] Guaraldo C., Lucherini V., De Sanctis E., Levi Sandri P., Polli E. and Reolon A. R., Lo Nigro S., Aiello S., Bellini V., Emma V., Milone C. and Pappalardo G. S. 1987 Phys. Rev. C 36, 1027.

[30] Jungerman J. A. and Steiner H. M. 1957 Phys. Rev. 106, 585.

[31] Terranova M. L., Kezerashvili G. Ya., Kiselev V. A., Milov A. M., Mishnev S. I., Protopopov I. Ya., Rotaev V. N., Shatilov D. N. and Tavares O. A. P. 1996 J. Phys. G: Nucl. Part. Phys. 22, 1661.

[32] Bianchi N., Deppman A., De Sanctis E., Fantoni A., Levi Sandri P., Lucherini V., Muccifora V., Polli E., Reolon A. R., Rossi M. Anghinolfi P., Corvisiero P. et al. 1993 Phys. Lett. B

299, 219.

[33] Cetina C., Heimberg P., Berman B. L., Briscoe W. J., Feldman G., Murphy L.Y., Crannell H., Longhi A., Sober D. I., Sanabria J. C. and Kezerashvili G. Ya., 2002 Phys. Rev. C 65, 044622.

[34] Frommhold Th., Steiper F., Henkel W., Kneissl U., Ahrens J., Beck R., Peise J. and Schmitz M. 1992 Phys. Lett. B 295, 28.

[35] Sanabria J. C., Berman B. L., Cetina C., Cole P. L., Feldman G., Kolb N. R., Pywell R. E., Vogt J. M., Nedorezov V. G., Sudov A. S., Kezerashvili G. Ya. 2000 Phys. Rev. C 61, 034604.

[36] Minarik E. V. and Novikov V. A. 1957 Sov. Phys. JETP 5, 253.

[37] Moretto L. G., Gatti R. C., Thompson S. G., Routti J. T, Heisenberg J. R., Middleman L. M., Yearian M. R. and Hofstadter R. 1969 Phys. Rev. 179, 1176.

[38] Ranyuk Yu. N. and Sorokin P. V. 1967 Sov. J. Nucl. Phys. 5, 37.

Figure Captions

Figure 1: Occupation number as function of single-particle level energy for the excited compound nucleus at the end of the intranuclear cascade, as calculated by the CRISP (full line) and the Liège-INC code (dashed line)[21]. We also show the occupation number for the ground state nucleus constructed by CRISP (dotted line).

Figure 2: Photoabsorption cross section per nucleon in the quasi-deuteron region. Experimental data (open squares) are taken from [26]. The CRISP results are indicated by full circles. The error bars are smaller than the symbols.

Figure 3: Neutron multiplicity in the quasi-deuteron region of photonuclear absorption. Experimental data (open squares) are taken from [27], and results from the CRISP code are marked as full circles. The error bars are smaller than the symbols.

Figure 4: Photofission cross section per nucleon for Bi and Pb target nuclei in the nucleon resonance region calculated by the CRISP code compared with experimental data. For Bi, the experimental data are taken from [28] (open squares), [29] (open triangles), [30] (open circles), [31] (open rhombs),[36] (open cross), [37] (open stars) and [38] (asterisks). For Pb, the data are taken from [33] (open squares).

Figure 5: Photofission cross section per nucleon in the Δ resonance region for various actinide targets. Experimental data are taken from [32] (open circles), [33] (open squares), [34] (open triangles), [35] (open rhombs). The full circles represent the results with the CRISP code. The error bars are smaller than the symbols.

Figure 1

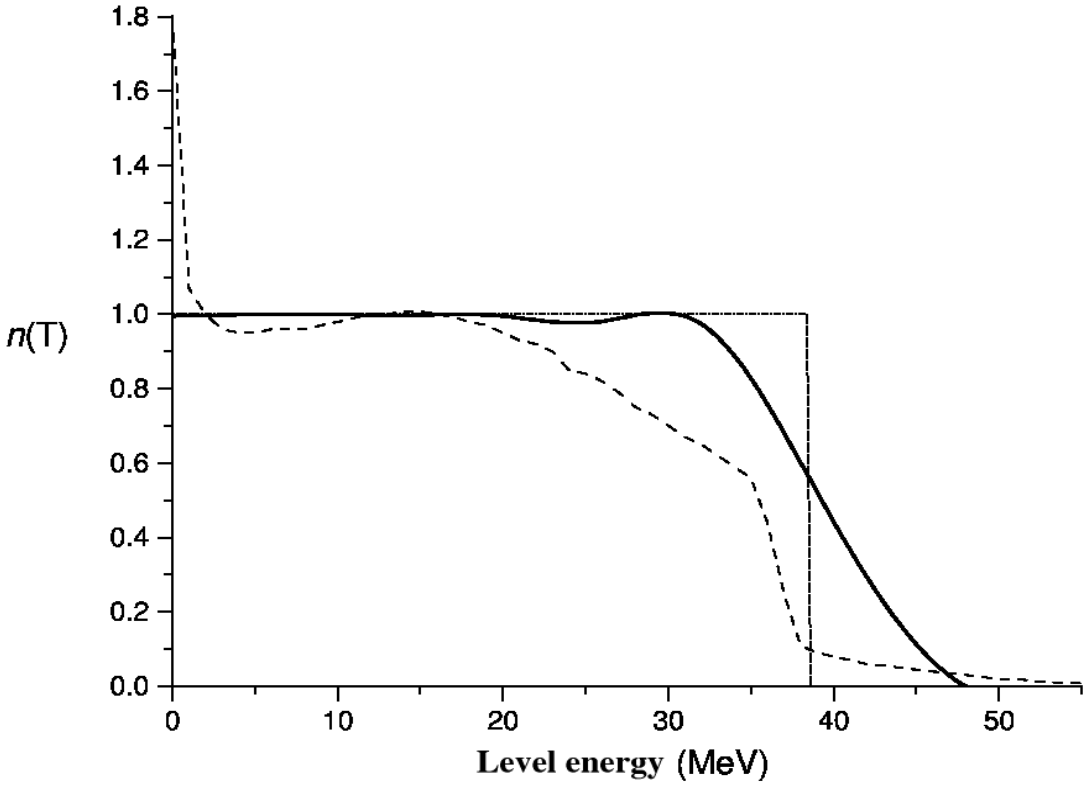

Figure 2

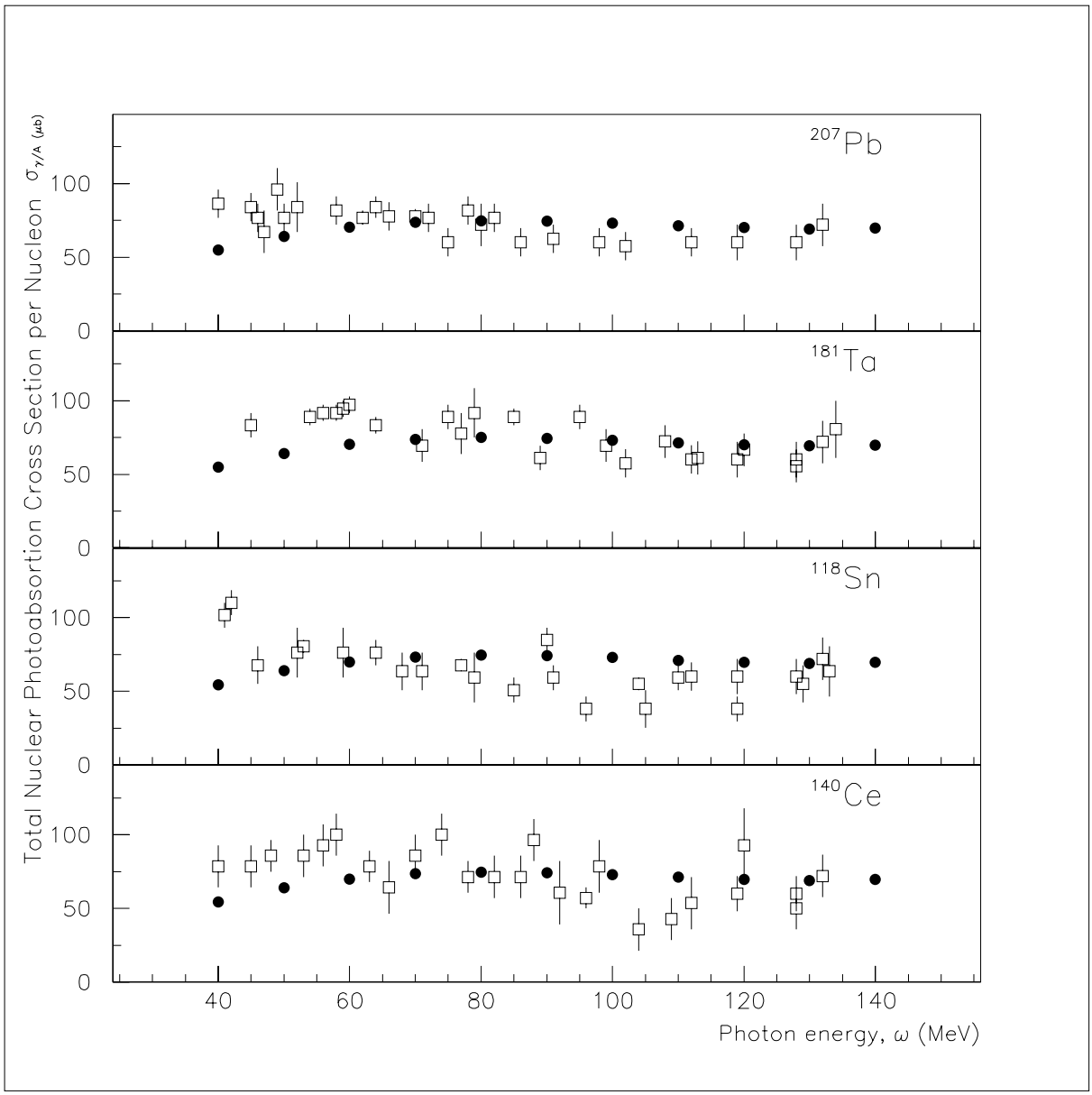
Total Nuclear Photoabsorption Cross Section per Nucleon $\sigma_{\gamma A}$ (μb)
^{207}Pb
^{181}Ta
^{118}Sn
^{140}Ce
0
50
100
40
60
80
100
120
140
Photon energy, ω (MeV)

Figure 3

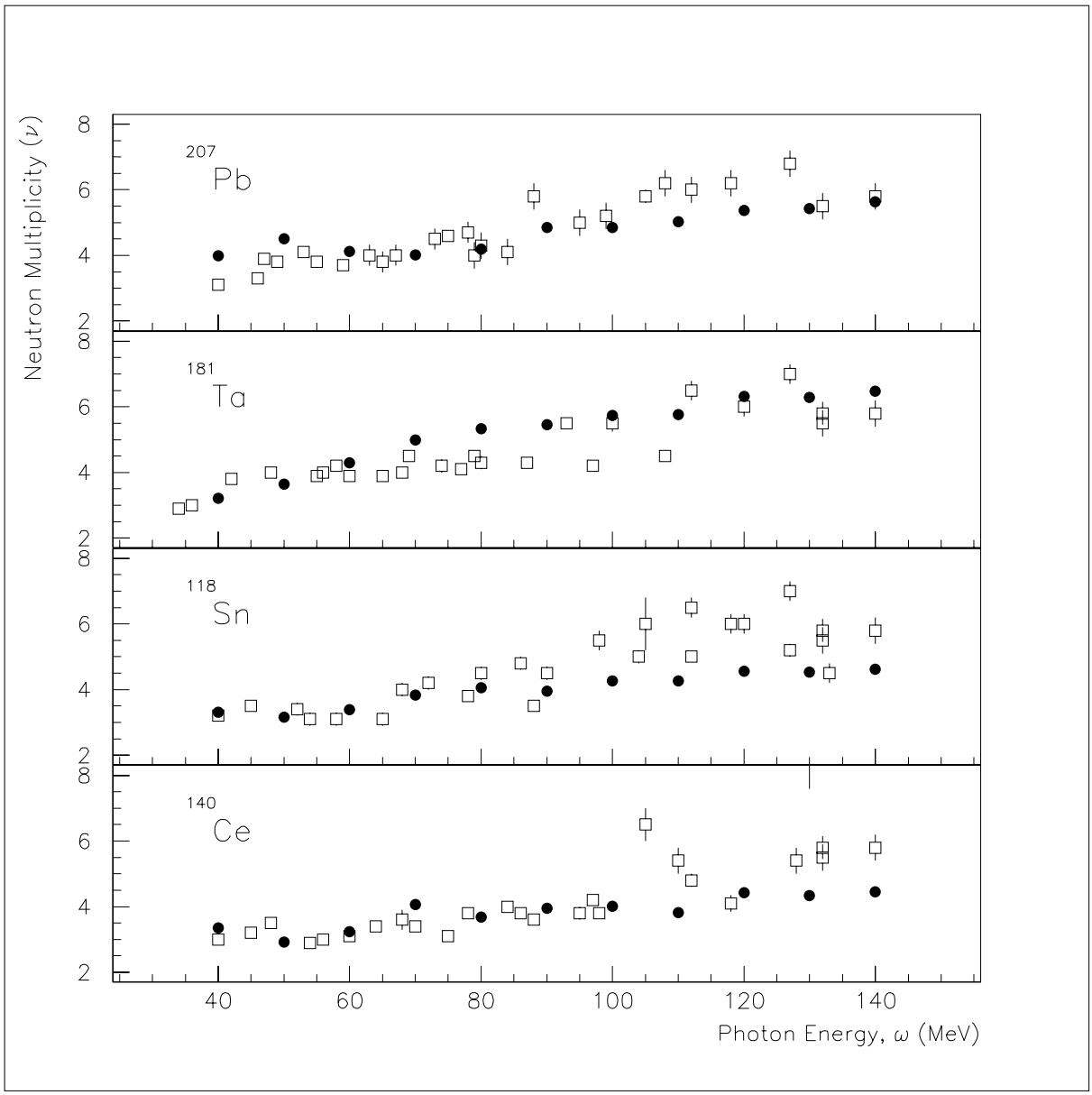
Neutron Multiplicity (ν)
207
Pb
181
Ta
118
Sn
140
Ce
2
4
6
8
40
60
80
100
120
140
Photon Energy, ω (MeV)

Figure 4

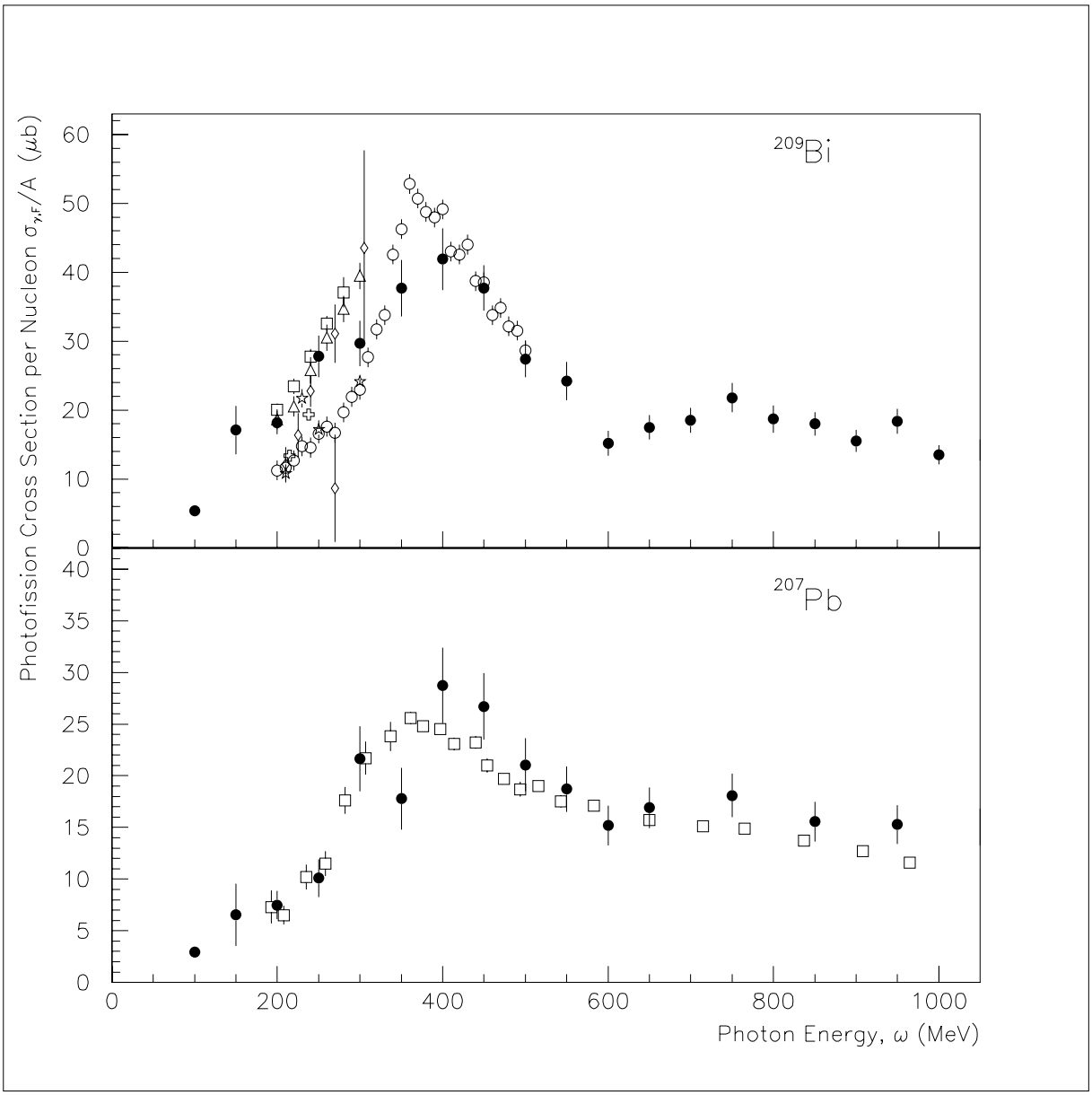
Photofission Cross Section per Nucleon $\sigma_{\gamma,F}/A$ (μb)
^{209}Bi
^{207}Pb
Photon Energy, ω (MeV)
0
10
20
30
40
50
60
5
15
25
35
200
400
600
800
1000

Figure 5

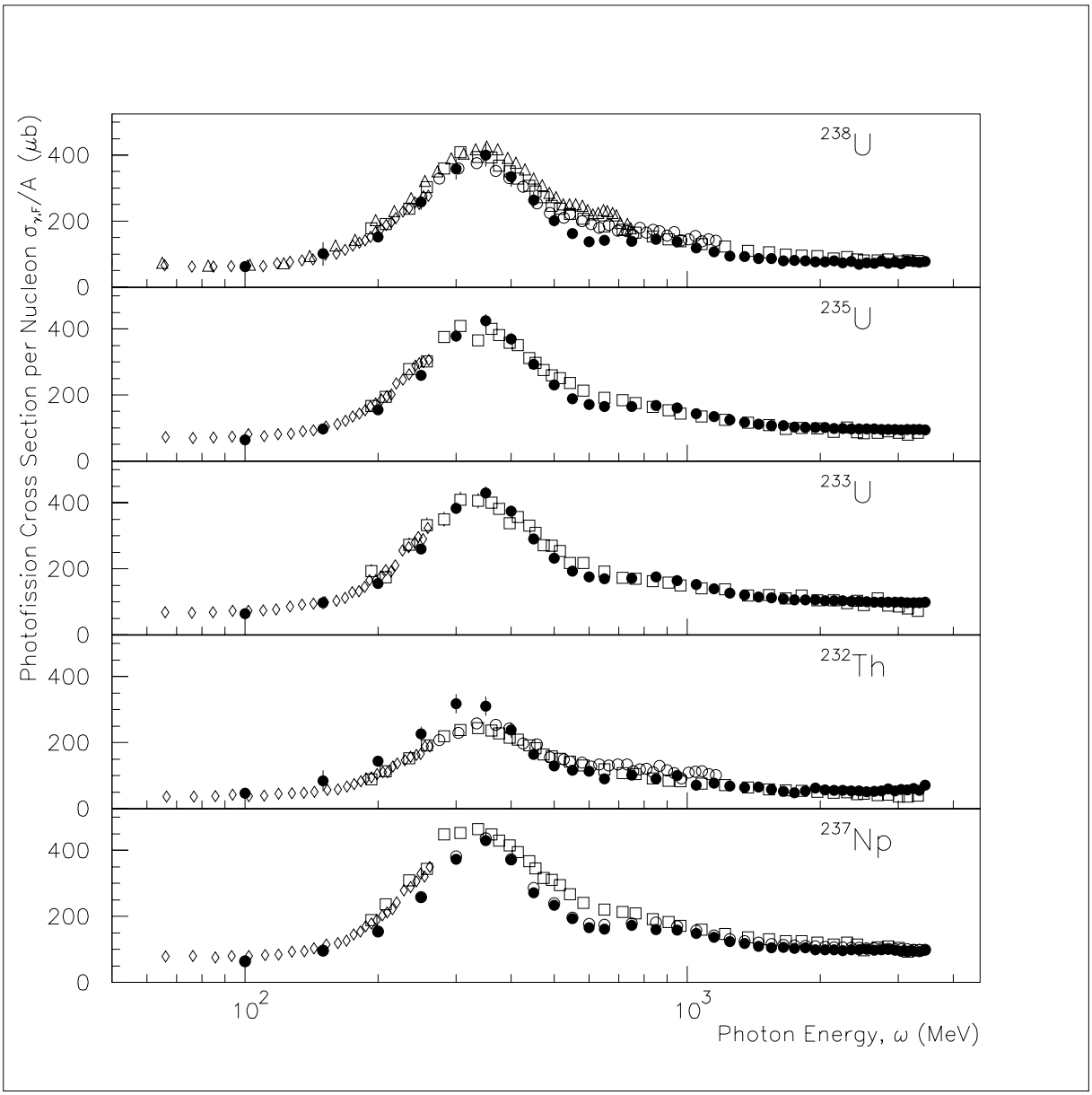
Photofission Cross Section per Nucleon $\sigma_{\gamma,F}/A$ (μb)
^{238}U
^{235}U
^{233}U
^{232}Th
^{237}Np
0
200
400
10^2
10^3
Photon Energy, ω (MeV)